THE JOURNAL OF PHYSICAL CHEMISTRY LETTERS
A JOURNAL OF THE AMERICAN CHEMICAL SOCIETY

pubs.acs.org/JPCL
Mini-Review

Perspectives on the Dynamic Nuclear Polarization Mechanisms of Monoradicals: Overhauser Effect or Thermal Mixing?

Frédéric A. Perras,* Frédéric Mentink-Vigier,* and Svetlana Pylaeva*

Cite This: J. Phys. Chem. Lett. 2025, 16, 3420−3432

ABSTRACT: This mini-review summarizes the evolving debate regarding the origins of the absorptive features seen in the dynamic nuclear polarization (DNP) spectra of certain monoradicals when they are irradiated at their electron Larmor frequency. This feature has drawn attention due to its reverse scaling with respect to the magnetic field strength and potential for high-field DNP. Two competing hypotheses have been introduced to explain the DNP feature based on (1) the Overhauser effect and low-temperature molecular dynamics and (2) radical clustering and a thermal mixing mechanism. Since the original discovery, a large number of experimental observations have been made in attempts to understand and ultimately leverage the mechanism. We summarize these observations and provide critical assessments of how the competing hypotheses approach them.

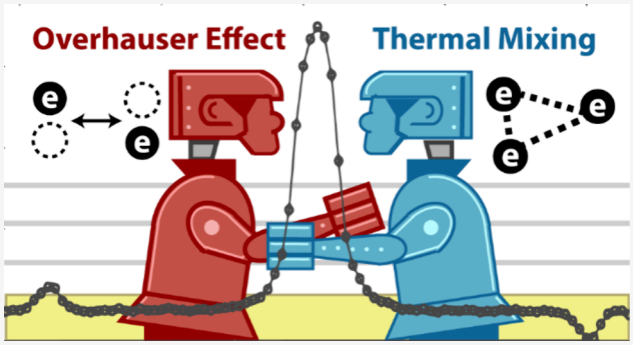

1. INTRODUCTION

Over the past two decades, dynamic nuclear polarization (DNP) has evolved into an important tool for studying the structure of materials, catalysts, pharmaceuticals, and biomolecules.[1−4] Specifically, DNP is used to enhance the sensitivity of nuclear magnetic resonance (NMR) spectroscopy by mediating a transfer of magnetization from electron spins to nuclear spins.[5] Because the electron's magnetic dipole moment is several hundred/thousand times stronger than that from a typical nuclide, the enhancements that are achieved can be quite transformative and enable previously unthinkable experiments. Modern DNP spectrometers operating at high magnetic fields commonly employ high-power continuous-wave (CW) microwaves (μw) (typically generated by vacuum devices)[6,7] to irradiate a particular allowed or forbidden electron paramagnetic resonance (EPR) to trigger a DNP mechanism. Different DNP mechanisms require different resonant conditions. This enables scientists to design paramagnetic systems, typically organic radicals, that will satisfy a particular condition or alternatively use field- or frequency-swept DNP measurements to determine the mechanism that is operational in a particular system.

There are four main mechanisms observed under continuous μw irradiation, namely, the Overhauser effect (OE),[8,9] the solid effect (SE),[10,11] the cross-effect (CE),[12] and thermal mixing (TM).[13] For given paramagnetic species, one mechanism or multiple mechanisms can act simultaneously, but each one requires specific conditions. For instance, the solid effect (SE) generates positive or negative DNP enhancements when saturating the forbidden electron−nuclear double- or zero-quantum transitions while the cross-effect (CE) instead requires two interacting electron spins whose frequency is separated by the nuclear Larmor frequency and the saturation of either of these electrons' EPR transition. Thermal mixing (TM) is conceptually similar to the cross-effect but instead relies on multielectron spin flips in an electron spin system that is homogeneously broadened by electron−electron couplings.[14] All three of the aforementioned solid state DNP mechanisms lead to positive enhancements when $\omega_{\mu w} < \omega_e$ and negative enhancements when $\omega_{\mu w} > \omega_e$[15−19] (Figure 1) and, under magic angle spinning, they rely on a coherent polarization transfer.[20,21]

The Overhauser effect (OE) is an incoherent mechanism that relies on electron−nuclear cross-relaxation. It was the first DNP mechanism to be postulated and observed but is less common in modern DNP as it requires fast modulation of electron−nuclear hyperfine couplings on the EPR time scale. The OE is typically associated with DNP in liquids[22,23] and conductors[8,9,24,25] where the electrons are mobile. Unlike the other three mechanisms, the OE effect only leads to a single extremum of either positive or negative sign, depending on the mechanism (Figure 1c; see also Theory).

Received: January 22, 2025
Revised: March 7, 2025
Accepted: March 10, 2025
Published: March 27, 2025

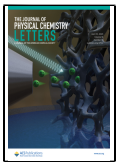

https://doi.org/10.1021/acs.jpclett.5c00225
J. Phys. Chem. Lett. 2025, 16, 3420−3432

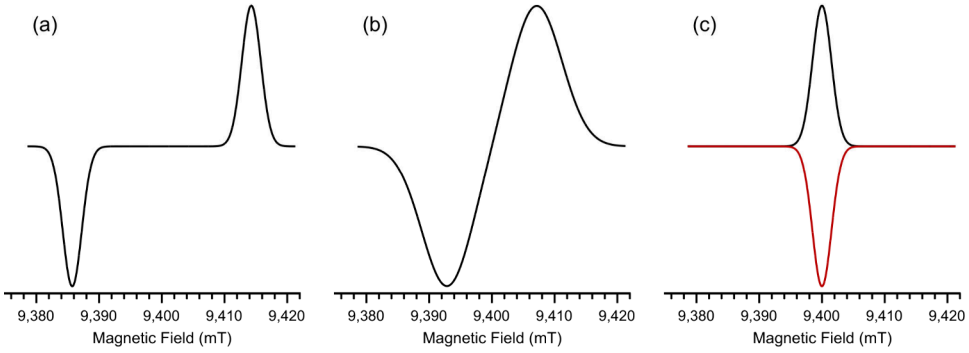

Figure 1. Simulated[18] DNP field sweep profiles expected for ^{1}H hyperpolarization in the case of (a) the SE, (b) the CE/TM, and (c) the Overhauser effect where the ZQ relaxation dominates (black) or the DQ relaxation dominates (red).

Up to 2014, it was generally thought that narrow-line ($\omega_n > \Delta\omega_e$) monoradicals dispersed in a dilute frozen solution primarily generate a solid effect DNP mechanism. However, a groundbreaking discovery in frozen solutions containing the BDPA monoradical challenged this understanding. For such samples, Can and co-workers not only observed the positive and negative SE DNP enhancements but also a constant positive sign enhancement when irradiating the EPR transition directly (see Figure 2).[26]

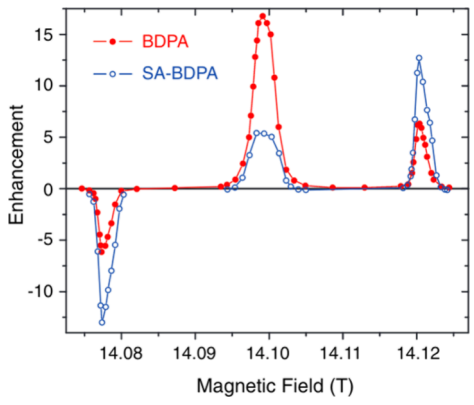

Figure 2. ^{1}H DNP enhancement profiles measured for solutions containing the BDPA and SA-BDPA radicals, displaying extrema from the solid effect mechanism in addition to a positive enhancement when the EPR transition is irradiated directly. Reproduced with permission from ref 26. Copyright 2014 American Institute of Physics.

Because the DNP field sweep profile agreed with only the generally accepted DNP matching condition of the OE, the feature was assigned to this mechanism. The authors attempted to explain the source of the effect by explaining that BDPA possesses large proton isotropic hyperfine couplings and assumed the existence of a modulation close to the electron spin Larmor frequency, which modulates the hyperfine couplings. The presence of such modulations was supported by the observed impacts of deuteration on the DNP enhancements and confirmed with simulations. This analysis was supported by the fact that the electron spins do relax (i.e., there exists a spectral density at the Larmor frequency of the electron spin), and they were able to use this argument to qualitatively simulate the experimental results. However, they failed to explain the molecular origin of the modulation. Later, a similar frequency profile was observed in a static sample at 1.2 K.[27]

This situation led to various groups proposing competing explanations for the observed phenomenon. Specifically, it was proposed that intramolecular vibrations, predicted by *ab initio* calculations, may be enough to modulate intramolecular hyperfine couplings and lead to cross-relaxation in BDPA (i.e., OE).[28,29] It was later demonstrated that strong electron−electron couplings in precisely arranged radical clusters can lead to unbalanced TM DNP, and a purely absorptive DNP field sweep profile, suggesting that the observed feature may instead originate from electron−electron interactions.[30]

Since the original 2014 publication,[26] new radicals have been observed to produce OE-like DNP field sweep spectra and numerous DNP and EPR experiments have been performed to attempt to distinguish the proposed mechanisms. The goal of this mini-review is to summarize the evidence that has been obtained in support of the competing models and provide an assessment of the current state of the debate. Considering the complexity of the discussion and the level of expertise required to understand the details behind each explanation, we will begin by summarizing the underlying theory behind the OE, CE, and TM mechanisms. We will then address each observation in turn and how they may be explained by the competing theories.

2. THEORY

In the following section, we briefly describe the competing mechanisms that have been postulated in contributing to the central absorptive DNP feature that is the focus of this mini-review. Specifically, these are the cross-effect, thermal mixing, and the Overhauser effect. The solid effect will not be described in detail as its signature, corresponding to enhancement observed at the conditions $\omega_e \pm \omega_n \approx \omega_{\mu w}$, is easily distinguished from the other mechanisms. The descriptions of the cross-effect and thermal mixing mechanisms are based on a recent description by Wenckebach.[14,31]

2.1. Cross-Effect. The cross-effect mechanism requires two ingredients: electron spins interacting with one another and a combined EPR line that encompasses the nuclear Larmor frequency. The irradiation of the allowed transition $\omega_{\mu w} = \omega_e$ generates a difference in the electron spin polarization. This polarization difference is transferred to the nuclei for the electron spins that obey the matching condition:[12,17,14,32]

$$\sqrt{\Delta\omega_{i,j}{}^2 + (2J_{i,j} + D_{i,j})^2} = |\omega_n| \quad (1)$$

The sign of hyperpolarization depends on whether the highest- or lowest-frequency electron spin is saturated. The description of this process is accurate for a three-spin system. In

https://doi.org/10.1021/acs.jpclett.5c00225
J. Phys. Chem. Lett. 2025, 16, 3420−3432

a real sample, where the concentration is on the order of tens of mM, the irradiation of the EPR line leads, by spectral diffusion, to the creation of a gradient of polarization across the EPR line. The polarization difference of each spin packet matching condition (1) can then be transferred to the nuclei. This mechanism is sometimes referred to as indirect cross-effect.[33−35]

Importantly, for the cross-effect, the EPR spectrum must be inhomogeneously broadened; i.e., the EPR line can be separated into spin packets which exchange polarization with one another through spectral diffusion. When this spectral diffusion is slow compared to the electron relaxation times, a gradient of polarization occurs between the spin packets and it is possible to "burn a hole" in the EPR line shape (see Figure 3). The

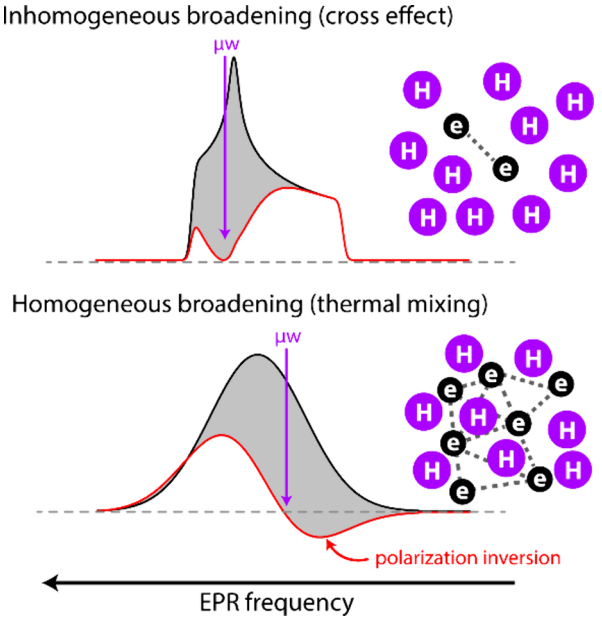

Figure 3. Example of the EPR spectra (black) and electron spin polarization under μw irradiation (red) in the cases of inhomogeneous broadening (top) and homogeneous broadening (bottom).

polarization difference of all spin packets matching condition (1) is then transferred to the nuclei through triple spin flips induced by the state mixing; however, not all spin packets will have the same polarization difference and it is not possible to define a single "non-Zeeman temperature" across the EPR line. Due to the relative size of the electron−electron couplings, the matching condition can often be accurately rewritten as.

$$|\Delta\omega_{i,j}| = |\omega_n| \tag{2}$$

2.2. Thermal Mixing. Thermal mixing[13] is a close sibling of the cross-effect in the sense that it requires electron−electron couplings to convert a polarization gradient toward nuclear hyperpolarization, and the two mechanisms have recently been presented in a unified framework.[14,31] The major difference between the cross-effect and thermal mixing is the rate of spectral diffusion, which is dictated by the strength of the interactions between electron spins. Thermal mixing occurs unequivocally when the EPR line is homogeneously broadened, which upon irradiation generates an electron non-Zeeman temperature that equilibrates with the nuclear spin reservoir: the thermal mixing consists in a flow of energy from the non-Zeeman energy reservoir. The thermal mixing condition can be approximated as

$$|2J_{i,j} + D_{i,j}| \approx |\omega_n| \tag{3}$$

In this regime, also dubbed "scrambled states",[17,36,37] rapid spectral diffusion leads to a mixing of electron polarization at a rate that surpasses longitudinal relaxation. As a result, the saturation of a packet of electron spins does not lead to a hole being burnt into the EPR line shape but rather an inversion about the frequency at which the saturation is applied (Figure 3).[38,39] Given that spectral diffusion is largely temperature independent while longitudinal relaxation is slowed at lower temperatures, TM is typically observed to be a more prominent mechanism at very low temperatures.[19] Similarly to the cross-effect, the polarization difference between electron packets separated by the nuclear Larmor frequency is transferred to the nuclear spins. When irradiation is applied in the center of the homogeneously broadened line shape, no net polarization difference is formed and no DNP enhancement is obtained; however, when irradiation is applied to either side of the EPR spectrum, the resulting polarization gradient is asymmetric and either a positive or negative enhancement is obtained, depending again on whether the high- or low-frequency side of the spectrum is irradiated.

Due to the extensive state mixing, the process can be viewed as a multielectron mechanism, while the cross-effect is most accurately described as a two electrons process. This distinction was made in recent work by Karabanov et al., who introduced a numerical model using only 3 electrons and a nucleus that exhibits thermal mixing.[40] In their article, the accent is placed on the fact that the dipolar coupling dominates the EPR spectrum and that for each electron spin, there must be an asymmetry in the dipolar couplings with the neighboring electron spins. The model developed by Karabanov et al. appears simple, yet powerful, as it could predict the behavior of trityl radicals displaying thermal mixing. While there is often debate on whether the TM or the CE is the dominant mechanism in a given sample,[19,41] it is generally agreed that TM occurs with trityls which present both a positive and negative lobe (Figure 4) close

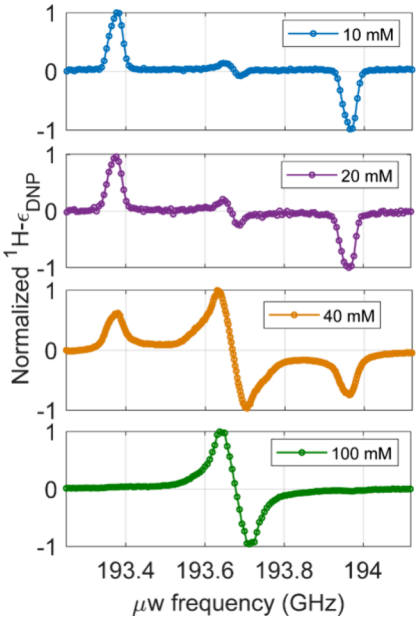

Figure 4. Increasing efficiency of thermal mixing of DNP as the radical concentration is increased for trityl radical solutions. Reproduced with permission from ref 42. Copyright 2020 American Chemical Society.

https://doi.org/10.1021/acs.jpclett.5c00225
J. Phys. Chem. Lett. 2025, 16, 3420−3432

to the EPR transition.[40,42] A new mechanism called resonant mixing has, however, recently been proposed as an alternative explanation.[43,44] For brevity, we will not cover resonant mixing or classical thermal mixing results in this mini-review.

2.3. Overhauser Effect. The OE was the first predicted and demonstrated DNP mechanism,[8,9] with observations being done with lithium metal. The mechanism requires the saturation of an allowed EPR transition, $\omega_{\mu w} = \omega_e$ and the existence of electron−nuclear cross-relaxation. More specifically, it relies on the existence of an imbalance between the characteristic relaxation time of the ZQ, $T_{1,ZQ}$, and DQ, $T_{1,DQ}$, transitions and nuclear polarization enhancement can be obtained if these rates differ (i.e., $T_{1,ZQ} \neq T_{1,DQ}$). The OE can be simulated by using a simple 1-electron-spin, 1-nuclear-spin system, whose Hamiltonian in the laboratory frame is given by

$$\hat{H}_0 = \omega_e \hat{S}_z - \omega_n \hat{I}_z + A^{iso} \hat{S}_z \hat{I}_z + 2A_z^{aniso} \hat{S}_z \hat{I}_z + A_+^{aniso} \hat{S}_z \hat{I}_+ + A_-^{aniso} \hat{S}_z \hat{I}_- \quad (4)$$

At high magnetic fields, this imbalance is due to the relative strengths of the isotropic, A_{iso}, and anisotropic, A_{aniso}, hyperfine interactions. If we assume that the DNP process relies on a second order effect (i.e., Redfield theory), the cross-relaxation rates are given by[45−47]

$$\frac{1}{T_{1,ZQ}} \propto (A_{iso}^2 + A_{aniso}^2/5) J_D(\omega_e - \omega_n) \approx (A_{iso}^2 + A_{aniso}^2/5) J_D(\omega_e) \quad (5)$$

$$\frac{1}{T_{1,DQ}} \propto \frac{3}{5} A_{aniso}^2 J_D(\omega_e + \omega_n) \approx \frac{3}{5} A_{aniso}^2 J_D(\omega_e) \quad (6)$$

where $J_D(\omega_e)$ is the spectral density of the fluctuation at the electron spin Larmor frequency. Importantly, modulations of the anisotropic hyperfine coupling accelerate DQ cross-relaxation, while isotropic hyperfine coupling modulations drive ZQ cross-relaxation, leading to opposite DNP enhancement signs depending on whether the cross-relaxation involves through-space or through-bond couplings.

All radicals that have been proposed to undergo OE DNP seem to utilize isotropic hyperfine coupling modulations due to electron or ^{1}H shuttling (see Sections 2.3.1 and 2.3.2). Given that these motions occur on a GHz time scale, nuclear Larmor frequencies are effectively shifted by several MHz. This could lead to a significant slowdown of the spin diffusion from these protons to the solvent ones. However, the protons on the radicals often possess various amounts of isotropic and anisotropic components, yielding a gradient of resonance shifts. This fact enables spectral overlap for protons on the radical and in the surrounding solvent. Under MAS the spin diffusion inside the radical and to the bulk is enabled by the nuclear dipolar rotor events.[48] Although this magnetization transfer has not been evaluated in detail, it has been postulated as a viable magnetization transfer path in the OE case.[49]

2.3.1. Mixed Valence Radicals. Mixed-valence (MV) molecules are compounds with degenerate ground electronic states. The molecules are well-known for their electron transfer properties.[29,50−53] They are commonly investigated experimentally by UV−vis spectroscopy and variable temperature EPR measurements, which provide estimates to the electron transfer rates. By changing the temperature, it is possible to transition from a high-temperature state, where two degenerate spin positions are equally populated, to a low-temperature state, where only one position is populated. Meaning that the exchange is slow in the EPR time scales. However, electron transfer processes can occur on a scale too fast to be resolved by currently available EPR setups,[54] but can provide an estimate for a lower limit of the electron transfer rate.

During the electron transfer process, spin density is shuttled between the two degenerate positions. This shuttling modulates isotropic hyperfine coupling constants because they are directly proportional to the electron spin density at the position of the nuclei.[28,29,55] These fluctuations occur at the frequency of electron transfer in MV compounds, potentially leading to ZQ electron−nuclear cross-relaxation and positive OE DNP enhancements. The electron transfer frequency is determined by the mechanism involved in the charge transfer. These can either be a charge transfer band, which is commonly found in the UV−vis range, or a quantum tunneling mechanism through the energy barrier separating the degenerate state energy along the electron transfer coordinate.

2.3.2. Methyl Dynamics. OE DNP mechanisms have also been proposed to occur in conjugated radicals containing methyl moieties.[49] In such systems, the spin densities on the methyl ^{1}H nuclei and thus their isotropic hyperfine couplings are dependent on the phase of the methyl group. Protons positioned along the node of a conjugated radical's spin density function will have zero hyperfine coupling, while those oriented perpendicular to the molecule's plane will typically have large isotropic hyperfine couplings. Motions of the methyl group thus lead to a modulation of the hyperfine coupling constant and in turn cross-relaxation.

The potential relevance of methyl rotations and librations as they pertain to Overhauser DNP were recently reviewed.[56] The rates of the motions have been evaluated using models based on the rolibrational wave function of a methyl group. These mechanisms can lead to dynamics in the hundreds of GHz time scale required for high-field OE DNP; however, these depend on the barrier for the rotation of the methyl group. For a 7-methyl functionalized Blatter radical system, both rotations and librations were found to lead to high cross-relaxation rates; however, the classical rotations could be frozen at ultralow temperatures. In a low-temperature regime, zero-point librations dominate the mechanism, which is conceptually similar to the mechanism proposed for mixed valence radicals.

3. EXPERIMENTAL OBSERVATIONS

In the following sections, we will summarize 10 observations that have been made regarding the observation of OE-like features in the DNP field sweep spectra of several monoradicals. When relevant, we summarize the approach used to reconcile the observations using the TM and OE hypotheses. A summary is presented at the end of the article.

3.1. Shape of the Field Sweep Profile. Most DNP mechanisms (SE, CE, and TM) feature multiple matching conditions of the microwave frequency relative to the EPR resonance frequency. This leads to either a positive or negative enhancement, depending on which condition is met. An illustration of the typical frequency profiles is shown in Figure 1. This is for instance observed in nitroxides,[5] but also in trityl for either ^{13}C or ^{1}H polarization.[40,42,44] The OE is perhaps unique in that it features only a single matching condition given that the population imbalance originates from relaxation processes rather than being driven directly by the application of μw irradiation. Observing these types of features in a DNP field

https://doi.org/10.1021/acs.jpclett.5c00225
J. Phys. Chem. Lett. 2025, 16, 3420−3432

sweep spectrum is thus considered to be a telltale sign of Overhauser effects.

Similar in-phase and on-resonance features are observed in the DNP frequency/field sweep profile of mixtures of carbon-centered and nitroxide radicals,[57] including in asymmetric biradicals of the same kind.[58,59] There, a positive DNP enhancement is observed when irradiating the narrower EPR resonance of the carbon centered radical due to the CE while the negative enhancement maximum is spread out over larger frequency ranges, often leading to negligible enhancement when low-power microwave sources are used. This observation of a lone positive enhancement maximum in radical mixtures or heterobiradicals was dubbed a Doppelgänger effect or truncated cross-effect (tCE).[60]

Li and co-workers showed in subsequent work that similar in-phase field sweep spectra can be obtained in a spin system featuring three monoradicals.[30] The model consisted of one radical molecule that is weakly coupled to a pair of strongly coupled radicals. The pair of strongly coupled BDPA molecules in the model provides the homogeneous broadening required to trigger the tCE and lead to a DNP spectral feature that mirrors the OE's signature (Figure 5).

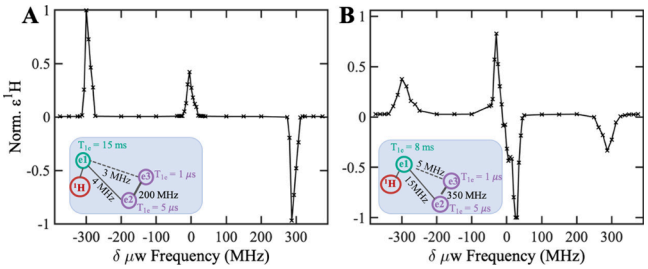

Figure 5. Simulations predicting an OE Doppelgänger effect in a DNP field sweep profile for a spin system containing a specific arrangement of three electrons and one nucleus (A). (B) Stronger electron−electron coupling leading to a dispersive line shape as observed in Figure 4. Reproduced with permission from ref 30. Copyright 2020 American Chemical Society.

A similar dipolar-based tCE was observed in the ^{13}C DNP of the P1 centers in diamonds. Shimon and co-workers observed extrema in their DNP frequency sweep profiles that lacked the dispersive features of the typical CE.[61] Opposite enhancement signs were observed depending on whether the EPR resonance associated with a ^{14}N spin in the $m = 1$ or -1 states was irradiated, disproving that this effect could be caused by an OE, which would maintain its sign. No such enhancement was observed when the central $m(^{14}N) = 0$ transition was irradiated, suggesting that the CE involved a central homogeneously broadened site. This site was later observed using EPR spectroscopy.[62] This experiment further highlights the sensitivity of the Doppelgänger effect, with respect to the resonance frequency of the broadened electron pair. Shimon's experiment further proves that dipolar-based tCE mechanisms are possible with narrow-line radical clusters.

Upon further study, Tobar and co-workers discovered that the production of the OE Doppelgänger at high fields would require inter-radical distances on the order of 5−6 Å that may not be geometrically feasible with organic monoradicals.[63] In molecular models focusing on electron−electron dipolar coupling alone, simulations predicted only the SE extrema. They then outlined the following two criteria required to produce an absorptive central DNP feature via electron−electron interactions: (1) electrons need to experience intermolecular coupling (dipolar and exchange interaction, J) with a strength equal to the nuclear Larmor frequency, and (2) the electron relaxation of the strongly interacting radicals needs to be rapid or otherwise a dispersive TM field-sweep spectrum is obtained.

For condition 1, the authors hypothesized that this strong intermolecular exchange coupling could be produced via a molecular docking mechanism initially proposed by Radaelli et al.[64] BDPA aggregation was justified from earlier work that showed the formation of covalent BDPA dimers as a major decomposition pathway.[65] The stability of such docked dimers, or their intermolecular exchange couplings, has yet to be investigated using quantum chemistry, and as such, it remains an open question whether this model can explain experimental observations. Docked dimers have not been observed either by crystallographic means or with use of electron microscopy.[66−68]

The second condition requires that the formation of pairs induces a significantly faster (~3 orders of magnitude) longitudinal relaxation of the electron spin. Currently, the evidence of this is limited. Strongly coupled biradicals often do not possess significantly shorter longitudinal relaxation times, as compared to their monoradical counterparts, except at very low temperatures.[69] As such, although it has been demonstrated that CE and/or TM can explain the observed DNP field sweep profiles in BDPA, further theoretical investigation is required to determine whether the outlined conditions can be satisfied in molecular models.

3.2. Asymmetric EPR Spectra. Li and co-workers observed that the EPR line shape produced when using high concentrations of BDPA together with low-power pulse EPR methods produces an asymmetric EPR line shape with an unusual appearance that may be expected from a hole-burning experiment (Figure 6a).[30] This asymmetry was claimed as a hallmark of TM DNP based on an earlier theoretical study published by Karabanov and co-workers.[40] This assertion appears to have been made in error. As mentioned in Theory, Karabanov et al. had identified that the coupling network needed to be asymmetric for TM to be allowed, not the EPR line shape. Specifically, for each electron spin, the sum of all of the dipolar couplings should not cancel out and the spin systems needed to contain both strong and weak electron−electron dipolar couplings to avoid the quenching of TM DNP (Figure 6b,c). Importantly, as with all purely dipolar-broadened line shapes, both scenarios that lead to successful and quenched TM DNP lead to perfectly symmetric EPR spectra. In a more recent publication, the group has identified the effect to instead be caused by instantaneous diffusion and not as evidence of TM DNP.[70,71]

3.3. Electron Hyperpolarization. TM DNP requires strong electron−electron dipolar couplings that ideally exceed the nuclear Larmor frequency in strength. Han and co-workers applied electron double-resonance (ELDOR) methods to look for strong electron−electron couplings in BDPA solutions.[30,72] They observed off-resonance electron hyperpolarization under continuous-wave irradiation which shows that (1) strong electron−electron dipolar couplings are present, (2) irradiation leads to the rise of an electron population imbalance between coupled spins, and (3) spectral diffusion is faster than the longitudinal relaxation, all of which are requirements for TM DNP (Figure 7b).

While these results do show that some major conditions required for TM DNP are met, they do not provide insights into

https://doi.org/10.1021/acs.jpclett.5c00225
J. Phys. Chem. Lett. 2025, 16, 3420−3432

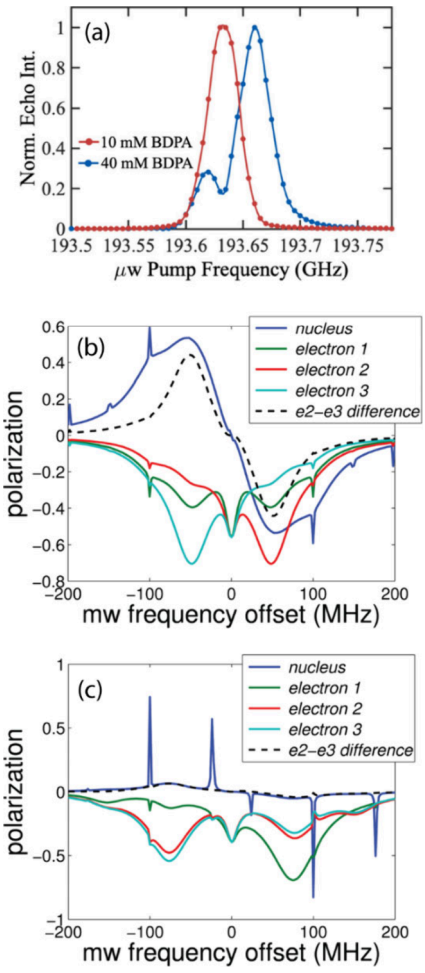

Figure 6. (a) Observation of asymmetric EPR line shapes under low-power microwave saturation. (b, c) Predicted DNP field sweep profiles (blue) and electron polarizations as a function of microwave irradiation frequency for asymmetric (b) and symmetric (c) coupling networks. While the asymmetric coupling network leads to TM DNP, the EPR line shape is symmetric. Panel a reproduced with permission from ref 30. Copyright 2020 American Chemical Society. Panels b and c reproduced with permission from ref 40. Copyright 2016 Royal Society of Chemistry.

how magnetization is transferred to nuclear spins. This point was made by Hovav and co-workers in 2015 when the effect was first observed.[33] They emphasized how the behavior of samples that are active toward TM DNP differs from that on conventional samples in hole burning EPR experiments. Samples that are active in TM DNP should display a 2-temperature behavior wherein the signal is inverted on one side of the irradiation frequency, rather than simply having a hole being burnt into the line shape (Figure 3),[13,38] as was observed experimentally by Atsarkin.[39] As such, they concluded that these effects could not be used as proof of TM DNP but instead are likely to be produced through coherent mechanisms. The transition between these two regimes was recently investigated by Caracciolo and co-workers[73] and Wenckebach.[74] Notably, in the intermediate regime, both hole burning and hyperpolarization are predicted, although the latter is only on one side of the irradiation frequency (Figure 7a). To expand on this, while the experiment disproves the existence of *classical* TM mechanisms, the presence of fast diffusion is not a requirement of the tCE, which is a coherent mechanism, and the experiment does confirm the existence of the strong electron−electron coupling that is required for the tCE mechanism.

3.4. Field Dependence. It is well established that the efficiency of the SE and CE mechanisms decreases with increasing magnetic fields due to the SE's second order nature[5,75] and the decreasing efficiency of MAS rotor events involved in CE MAS DNP.[21,76,77] By its nature, TM relies on the same interactions as CE and is thus expected to feature decreasing performance with increasing magnetic field strengths. TM's efficiency also depends on the magnetic field independent electron−electron dipolar couplings being of comparable magnitude to the nuclear Larmor frequency, and as such, it is anticipated that at high fields the TM mechanism would be quenched and superseded by the CE.

In 2014, Can and co-workers reported the observation of an increase in OE DNP performance as a function of increasing magnetic field strength.[15] The OE mechanism successfully explains this observation. BDPA is a MV radical with predicted vibronic transitions occurring at a frequency of approximately 600 GHz.[28] Calculated spectral density functions for this radical display a broad peak centered at this frequency with substantial intensity present over a wider range (Figure 8). As a result,

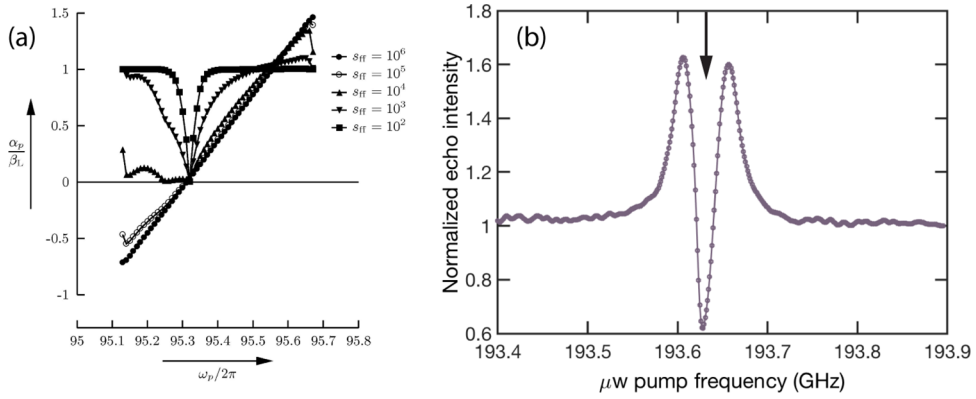

Figure 7. (a) Numerically calculated electron polarization, normalized to the thermal polarization, for an ensemble of TEMPO radicals as a function of the spectral diffusion frequency, showing the transition from a hole-burning regime to the two-temperature regime associated with thermal mixing. (b) Analogous experiments performed on a 40 mM OTP solution of the BDPA radical at 15 K showing off-resonance electron hyperpolarization but no two-temperature behavior. Panel a reproduced with permission from ref 74. Copyright 2017 Elsevier. Panel b reproduced with permission from ref 72. Copyright 2024 American Chemical Society.

https://doi.org/10.1021/acs.jpclett.5c00225
J. Phys. Chem. Lett. 2025, 16, 3420−3432

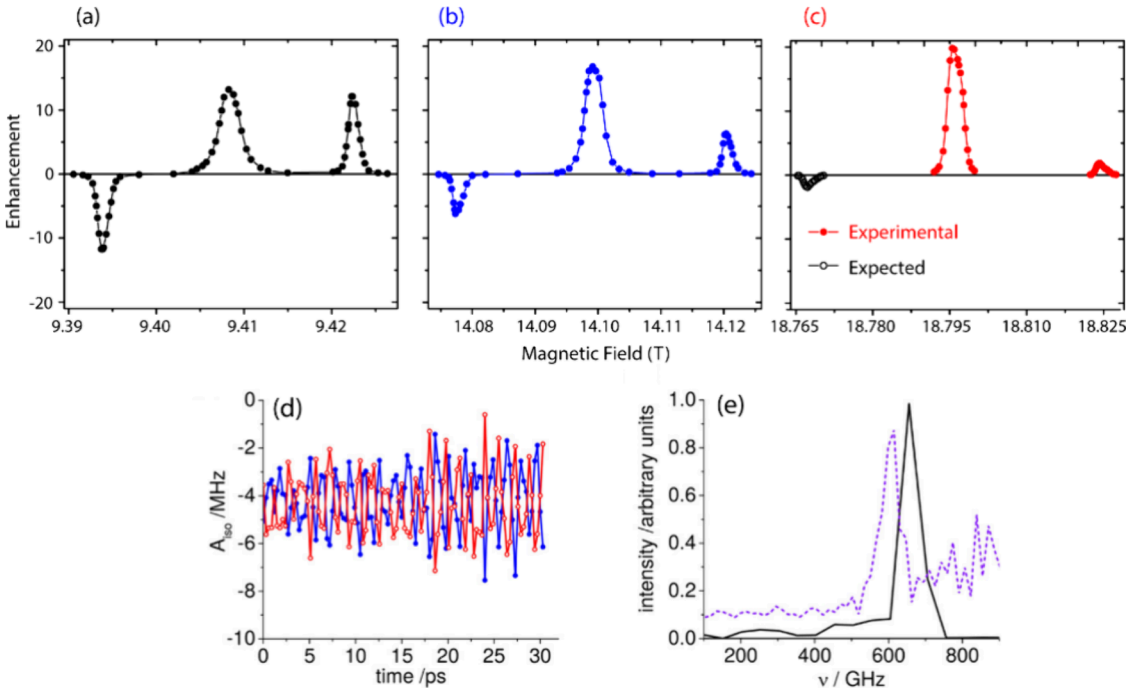

Figure 8. DNP field sweep profiles measured for a BDPA solution as a function of the applied magnetic field strength: (a) 9.4 T, (b) 14.1 T, and (c) 18.8 T. Predicted time dependence of A_{iso} in BDPA (d) and the corresponding spectral density function (e) calculated using an *ab initio* vacuum model (black) and a classical MD trajectory for a frozen OTP matrix (purple). Panels a– c reproduced with permission from ref 26. Copyright 2014 American Institute of Physics. Panels d and e reproduced with permission from ref 28. Copyright 2018 American Chemical Society.

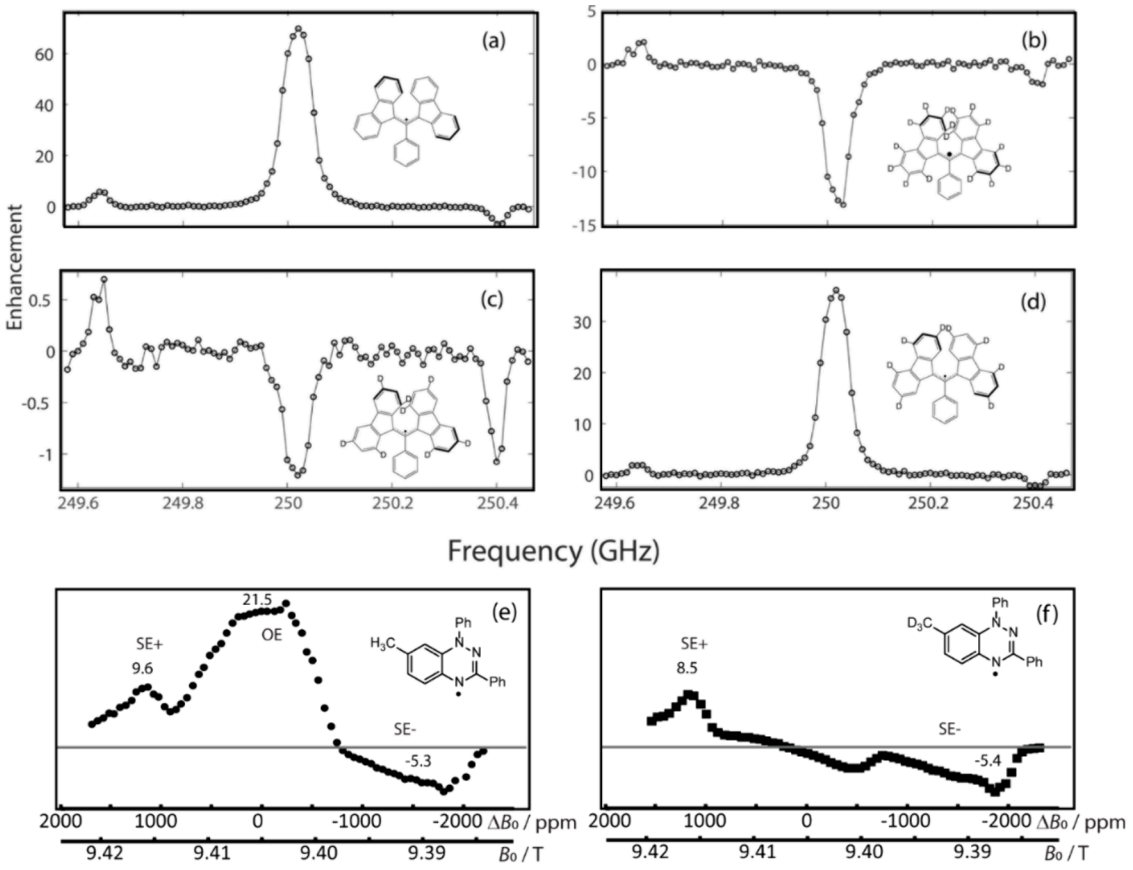

Figure 9. DNP field sweep spectra measured for varied selectively deuterated BDPA variants (a–d) and methyl-functionalized Blatter variants (e, f). Panels a–d reproduced with permission from ref 81. Copyright 2021 American Chemical Society. Panels e and f reproduced with permission from ref 49. Copyright 2022 American Chemical Society.

https://doi.org/10.1021/acs.jpclett.5c00225
J. Phys. Chem. Lett. 2025, 16, 3420–3432

$J_D(\omega_e)$ (see eqs 3 and 4) increases with increasing magnetic field strength and cross-relaxation rates thus increase. It is important to note, however, that this vibrational mode has not thus far been detected by THz spectroscopy and has not been experimentally verified.

Mathies and co-workers have studied the field dependence of the DNP performance of a series of heterobiradicals known as TEMTriPols.[58] For two of the four variants studied, they observed a higher performance at 14.1 T, as compared with 5 T, while lower performance was always observed at 18.8 T. As described in Section 3.1, these radicals utilize the CE (or tCE) mechanism, providing some evidence that tCE performance may increase at higher magnetic field strengths. As such, the observed increase in efficiency with increasing magnetic field seen with BDPA may be consistent with a tCE mechanism. It is nevertheless important to state that the proposed broadening mechanism for the BDPA site with a larger EPR line width differs from that in TEMTriPol (electron dipolar couplings vs g anisotropy)[78] and that a dipolar-based tCE mechanism may display decreased efficiency at fields where the electron dipolar couplings are weaker than the nuclear Larmor frequency. To the best of our knowledge, explicit spin dynamics simulations have not been performed to confirm whether the tCE model yields the observed field dependence.

3.5. Polarization Time. In all three classes of systems where an absorptive DNP central feature was observed (BDPA, mixed-valence diamines, and 7-CH_3 Blatter),[15,49,79] the DNP buildup times were found to be essentially limited by the nuclear T_1 relaxation times and comparable to the SE DNP buildup times. Both SE and OE DNP mechanisms are expected to be slow processes, being limited by the time required to saturate a forbidden transition.[16,80] On the other hand, the CE and TM are typically highly efficient and yield fast nuclear polarization buildup times.[17,14,31,80] Although these observations may appear to refute the CE/TM hypothesis, a slow buildup may be consistent with a sample composed of passive clusters of radicals and low concentrations of DNP-active isolated, weakly coupled radicals (Section 3.1). These may, for instance, be detected as a nonlinear dependence of the EPR signal intensity on the radical concentration; however, this experiment has, to the best of our knowledge, not yet been performed. Whether a TM theory involving asymmetric radical distributions can indeed replicate the observed slow buildup times remains to be seen.

3.6. Deuteration Experiments. The OE is most sensitive to electron−nuclear coupling interactions (and their modulation), while TM is instead mainly controlled by electron−electron coupling interactions (refer to Theory). As described in eqs 3 and 4, isotropic hyperfine coupling-dominated cross-relaxation would lead to faster ZQ relaxation and a positive DNP enhancement, while dipolar-dominated cross-relaxation leads to faster DQ cross-relaxation rates and a negative DNP enhancement. Deuteration experiments are thus highly informative in allowing the differentiation of the two mechanisms given that while deuteration will not impact radical clustering, it can remove cross-relaxation partners that may be responsible for OE DNP.

In their seminal study,[15] Can et al. tested fully protonated and perdeuterated BDPA variants. The removal of the protons on BPDA-d_{21} eliminated all intramolecular isotropic hyperfine interactions, leaving only dipolar coupled solvent protons. In so doing, they observed a change in DNP enhancement sign commensurate with a transition from ZQ- to DQ-dominated cross-relaxation, yielding experimental results matching the simulations. This could further be replicated if only the strongly hyperfine coupled sites were deuterated (Figure 9).[81]

Most recently, Palani and co-workers pushed the deuteration scheme further to identify which protons are most affecting the enhancement at the center of the DNP profile.[82] They showed that by deuterating the dipolar-coupled phenyl ^{1}H's, they could reduce the DQ cross-relaxation contribution, thus enhancing the magnitude of the OE enhancement factors (Figure 9). DFT calculations further revealed strong isotropic intramolecular hyperfine couplings between specific ^{1}H nuclei and the electron spins that were also shown to be dynamically modulated via vibronic coupling. The site-specific deuteration of these ^{1}H's alone was shown to be sufficient to eliminate the positive OE DNP maximum.

Similar deuteration experiments were performed in the 7-CH_3−Blatter radical system.[49] The site specific deuteration of the methyl ^{1}H's alone eliminated the OE feature, while the efficiency of the SE DNP was unaffected (Figure 9). Despite not yielding a ^{1}H OE DNP feature, however, the 7-CD_3−Blatter radical was highly efficient in ^{2}H OE DNP.

Both CE and TM rely primarily on electron−electron dipolar or exchange coupling interactions that are independent of isotopic labeling. They should thus respond similarly to the SE mechanism when a radical is deuterated. The predicted sign of the Doppelgänger effect, is further solely determined by the geometry of the electron spin clusters and thus should not be inverted through deuteration.[30,70] As of now, no explanations have been put forth that could explain the site specificity of the effect using a TM model or why it changes in sign as a result of specific site deuteration. Current models would suggest that any labeling strategy that would quench the TM should also similarly quench the SE, which was not observed.

3.7. Microwave Power Dependence. In the case of BDPA, the Blatter systems, and diamine radicals,[15,49,79] the central feature was shown to saturate at lower microwave powers than the SE extrema. All three mechanisms considered, TM, CE, and OE involve the saturation of allowed EPR transitions which are more easily saturated than the forbidden transitions involved in the SE. As such, the observed power dependence is consistent with both models.

3.8. Temperature Dependence. The central absorptive feature in the DNP field sweep spectra of both 7-CH_3−Blatter and BDPA have been studied down to temperatures of 18 and 1.2 K, respectively.[27,56] In both cases, a higher performance was observed at lower temperatures, which would seem at a glance to disprove the OE hypothesis given that it requires molecular motions. Pylaeva and co-workers have, however, shown that the OE is caused predominantly by vibronic transitions (zero-point vibrations).[28,29] These motions do not freeze and continue to provide a mechanism for OE DNP down to 0 K. In the 7-CH_3−Blatter example, Perras and co-workers studied the expected behavior from methyl rotation, libration, and tunneling;[56] while at 100 K methyl rotations can lead to considerable OE, at temperatures below 50 K zero-point methyl librations dominate. Gains in enhancement predominantly arise due to the lengthening of the nuclear and electron relaxation times. As such, both the TM and OE hypotheses can explain the temperature dependence of the effect, with the main contribution stemming from relaxation times.

Tobar and co-workers studied the temperature dependence of the ^{1}H DNP field sweep profiles from very high concentrations of SA-BDPA (Figure 10).[63] The stability of the radical appears to be modest, and the authors used a very high 300 mM

https://doi.org/10.1021/acs.jpclett.5c00225
J. Phys. Chem. Lett. 2025, 16, 3420−3432

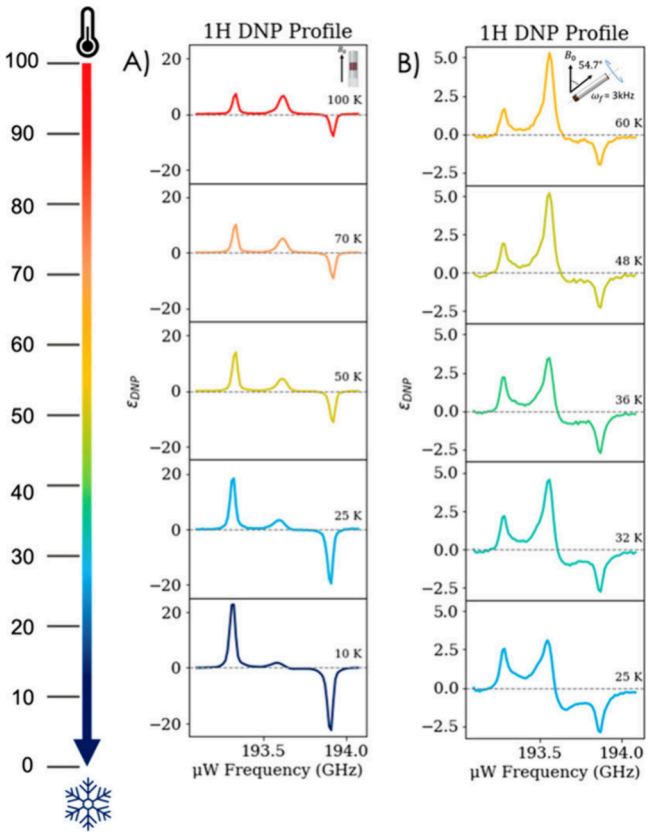

Figure 10. DNP frequency sweep profiles measured for a highly concentrated BDPA solution as a function of temperature, as indicated in the image, for both static (A) and spinning (B) samples. Reproduced with permission from ref 63. Copyright 2023 American Chemical Society.

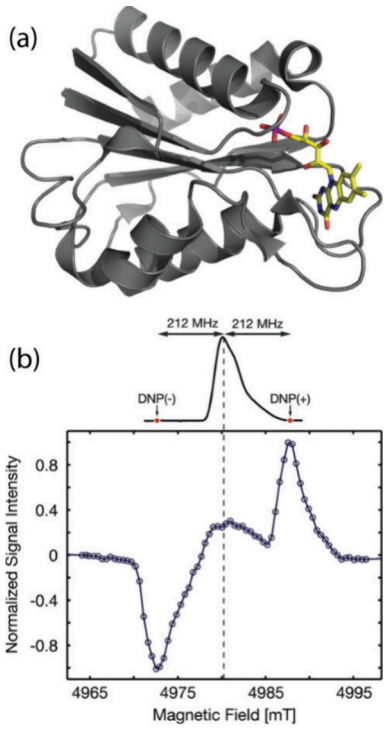

Figure 11. (a) Ribbon structure of the flavodoxin protein showing the location of the methyl-functionalized radical moiety. (b) High-field EPR spectrum of the protein and its corresponding DNP field sweep profile displaying a positive DNP maximum when the EPR transition is irradiated. Reproduced with permission from ref 83. Copyright 2010 American Chemical Society.

concentration of solute to have an effective concentration close to ∼60 mM electron spins. At temperatures below 45 K, they clearly observed both positive and negative enhancement regions when irradiating the EPR single-quantum transition, with the positive lobe remaining the most intense. This observation is best explained by a superposition of the OE and TM mechanisms in a highly concentrated solution. As mentioned earlier, the TM mechanism gains in prominence at lower temperatures.[19]

3.9. Flavodoxin. Although first identified by Perras in 2022,[49] methyl-driven OE may have been first reported by Maly and co-workers in 2012 while studying DNP in flavodoxin.[83] The protein contains a conjugated radical with methyl functionalization, not unlike the 7-CH_3–Blatter system. As can be seen in Figure 11, a positive feature was observed in the DNP field sweep spectrum upon irradiation of the EPR transition directly. Due to the size of the protein (∼20 nm), the maximum intermolecular electron–electron dipolar couplings of ∼6 kHz are far too low in comparison with the ^{1}H Larmor frequency (212 MHz) to lead to TM.

Considerable literature, however, exists on the topic of the spin density functions in flavoproteins, the hyperfine couplings to the methyl protons, and the rapid rotational dynamics of the methyl groups.[84−86] These studies revealed that the isotropic hyperfine couplings to the 8-CH_3 protons are particularly sizable, on the order of 20 MHz,[87,88] and that the methyl groups behave as quantum rotors.[88] From their measured 280 MHz tunneling frequency, we calculated a 1700 GHz librational frequency,[89] which would be consistent with the observed weaker OE maximum, as compared to the Blatter system.

3.10. Polarizing Agent Design. The proposed mechanisms aimed at explaining the absorptive central DNP feature require extremely different criteria to be efficient. Both of these have been targeted for the synthesis of new or improved DNP polarizing agents that would function either through TM or OE. One such successful example was mentioned in Section 3.6. wherein Palani and co-workers selectively deuterate dipolar, but not isotropically hyperfine, coupled hydrogen atoms on BDPA to reduce the DQ cross-relaxation rate and improve the positive OE enhancement.[82]

Inspired by the idea that MV radicals could be used to unlock the OE mechanism, Gurinov and co-workers investigated the application of MV diamine radicals.[79] The electron transfer rate in this system was previously estimated to be on the order of 100 GHz,[54] which is in the range required for high-field OE DNP. The diamine radicals indeed produced a positive DNP enhancement when irradiating directly at the electron Larmor frequency and even surpassed BDPA in terms of performance (Figure 12). Furthermore, given that the radicals hold positive charges, it is particularly unlikely that they would cluster.

A similar attempt at designing a purpose-built TM polarizing agent was recently presented by Chaklashiya and co-workers who tethered together four trityl radicals in order to force clustering.[70] While the radical did produce significant TM at low concentrations (5 mM), the majority of the effect was found to be driven through intermolecular couplings. The radical also produced the typical positive and negative TM extrema observed with Trityl, and no Doppelgänger effect.[40,42]

https://doi.org/10.1021/acs.jpclett.5c00225
J. Phys. Chem. Lett. 2025, 16, 3420−3432

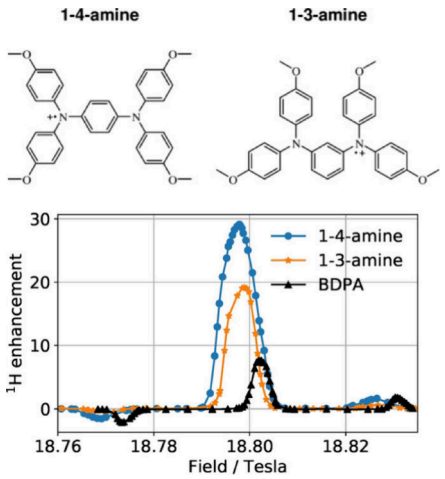

Figure 12. Structures of the 1,4- and 1,3-amine MV radicals designed for OE DNP (top) and their corresponding DNP field sweep profiles, displaying larger positive maxima when the fundamental EPR transition is saturated (bottom). Reproduced with permission from ref 79. Copyright 2021 John Wiley & Sons.

3.11. Complexity. The previous ten sections intend to summarize the main observations that have been made to understand the positive central DNP maxima observed with BDPA, and other radicals, and the corresponding explanations that were presented as they relate to TM and OE models. There is, however, one less substantive point that we believe warrants further scrutiny.

As was briefly touched on in Section 3.1, the level of complexity required to produce an absorptive central DNP feature via TM, and the sensitivity of the simulations to the input parameters, is large. Specifically, the model requires a pair of strongly exchange coupled electron spins that are weakly coupled to a third spin, with the exchange coupling constant equal to the nuclear Larmor frequency. Slight deviations in the model lead to dispersive TM DNP field sweep spectra.[30,70] To date, no estimates have been made regarding the stability or probability of the proposed arrangement existing at low temperatures nor whether such strong intermolecular exchange coupling interactions are indeed feasible. The OE model is at a basic level far simpler, and sensible models based on quantum chemistry have shown that absorptive features can be produced in 1-electron systems. Occam's razor therefore greatly favors the OE hypothesis in this regard.

Demonstrating that the TM model is indeed chemically sensible would require a substantial experimental and theoretical study. To this aim, it is essential to recognize that radicals often have complex electronic structures. BDPA for instance, is not well described using DFT.[29] Complexities arise from the multireference character of the molecule, where its ground state is represented not as a single well potential but as a double-well potential along the electron transfer coordinate. Although specific DFT functionals such as BLYP35 and BMK were developed to address MV compounds, even these functionals tend to overestimate vibronic coupling in BDPA, resulting in a fully symmetric C_{2v} structure. The explicit inclusion of a number of excited states is necessary. For BDPA, CASSCF(3,3) calculations yield qualitatively correct results, providing an accurate ground state geometry for the radical.

4. SUMMARY

To recapitulate, the purpose of this mini-review has been to summarize the observations that have been made to elucidate the DNP mechanism that leads to the absorptive DNP field sweep profile feature observed when irradiating the fundamental EPR transition in a growing number of radicals (Figure 13).

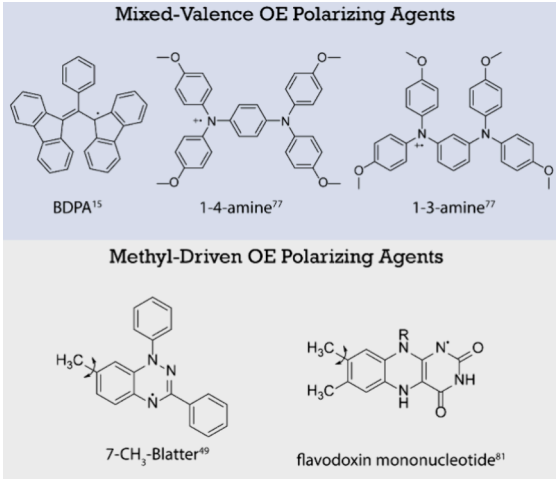

Figure 13. Radicals that have been shown to display OE-DNP-like behavior. These are distinguished by the type of motions present, namely, vibration-like electron shuttling in mixed-valence radicals (top) and methyl rolibrational dynamics (bottom). References to their first observations are noted on the image.[15,49,77,81]

Given that the mechanism has demonstrated potential for high-field DNP, identifying its origins is the first step toward the development of next-generation polarizing agents. In the preceding section we have outlined the 10 observations that have been made and how these are addressed by models based on the Overhauser effect and thermal mixing and/or cross effect. These have been summarized in Figure 14 below, together with our assessments.

In short, the strongest arguments made in favor of the TM model involve the observation of strong electron−electron dipolar couplings in solutions containing BDPA radicals. These are seen to lead to electron hyperpolarization when irradiating the EPR transition with off-resonance microwaves, which imply that the dipolar interactions are strong and crucially stronger than the electron longitudinal relaxation time, a key requirement of the TM model. An asterisk has been placed in Figure 14 for this point given that while this implies the existence of strong electron−electron dipolar interactions, the experiment disproves the formation of a 2-temperature electron spin system typically associated with TM. Given that the model does not generally implicate classical TM theory, this should not be seen as a falsification of the theory.

While the TM model has yet to be successfully applied in radical design, ideas based on the OE model have led to the development of better performing polarizing agents. It is nevertheless conceivable that a TM-based model could, with further study, achieve a similar feat.

Regarding the DNP field sweep profile, this is seen to be fully consistent with OE theory and indeed predicted by quantum chemical calculations of electron hyperfine couplings and molecular dynamics. While the TM model can replicate this observation, it requires complex models that are not chemically feasible. Further study would be required to determine whether

https://doi.org/10.1021/acs.jpclett.5c00225
J. Phys. Chem. Lett. 2025, 16, 3420−3432

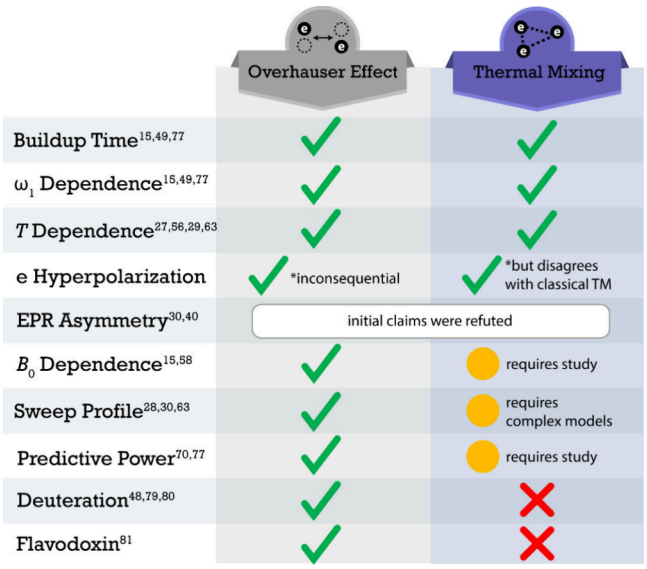

Figure 14. Overview table summarizing which observations are currently well explained by the OE and TM models. Asterisks are used to highlight specific noteworthy details to green checkmarks. Yellow circles identify observations that have yet to be reconciled by a theory and require further study. Red crosses highlight observations that are unlikely to be explained by a theory. Readers are referred to the text in Section 3 for details. Key references are given in the leftmost column.

the proposed intermolecular exchange coupling interactions and differences in relaxation times can be produced in stable molecular models.

Two of the 1 observations, however, have a low likelihood of ever being reconciled with the TM model. Specifically, in both BDPA and methyl-functionalized Blatter radicals, the site-specific deuteration of the protons predicted by quantum chemistry to have modulated hyperfine interactions was seen to quench the OE maximum. Furthermore, in the latter system, this deuteration was seen to activate the ^{2}H OE mechanism while leaving the ^{1}H SE mechanism unphased. The deuteration of all protons in BDPA was further seen to lead to an apparent shift from through-bond to through-space OE mechanisms. Given that the TM model depends primarily on the arrangement of the electron spins, a variable that is held constant in isotope labeling experiments, we do not see a path whereby TM theory would predict such quenching (or reversal of sign) of the mechanism, particularly while the SE performance is unaffected. The second observation is the apparent detection of methyl-driven OE DNP with a monoradicals encapsulated inside of a large protein. There, the intermolecular dipolar interactions are estimated to be at most 6 kHz in magnitude: 5 orders of magnitude too low to satisfy to the TM matching condition.

As such, we conclude by stating that while conclusive TM DNP has been observed in concentrated BDPA solutions,[63,90] observations made to study the absorptive central DNP feature in mixed-valence radicals and methyl-containing conjugated radicals are only explained by an OE mechanism. While additional computational work could be done to show that a molecular cluster can lead to such an effect, the OE mechanism is the only mechanism that explains the performance at high fields, in deuterated systems, and encapsulated radicals where clustering is not possible.

AUTHOR INFORMATION

Corresponding Authors

Frédéric A. Perras − *Chemical and Biological Sciences Division, Ames National Laboratory, Ames, Iowa 50011, United States; Department of Chemistry, Iowa State University, Ames, Iowa 50011, United States*; Email: fperras@ameslab.gov

Frédéric Mentink-Vigier − *National High Magnetic Field Laboratory, Florida State University, Tallahassee, Florida 32310, United States; Department of Chemistry and Biochemistry, Florida State University, Tallahassee, Florida 32306, United States*; orcid.org/0000-0002-3570-9787; Email: fmentink@magnet.fsu.edu

Svetlana Pylaeva − *Department of Chemistry, University of Paderborn, 33098 Paderborn, Germany*; orcid.org/0000-0002-7315-2932; Email: pylaeva@mail.uni-paderborn.de

Complete contact information is available at: https://pubs.acs.org/10.1021/acs.jpclett.5c00225

Notes

The authors declare no competing financial interest.

ACKNOWLEDGMENTS

F.A.P. was supported by the U.S. Department of Energy (DOE), Office of Science, Basic Energy Sciences, Materials Science and Engineering Division, Materials Chemistry. Ames National Laboratory is operated for the U.S. DOE by Iowa State University under Contract No. DE-AC02-07CH11358. The National High Magnetic Field Laboratory (NHMFL) is funded by the National Science Foundation Division of Materials Research (DMR-2128556) and the State of Florida. S.P. thanks Deutsche Forschungsgemeinschaft (DFG) for funding (PY 117/1-1:1).

REFERENCES

(1) Biedenbänder, T.; Aladin, V.; Saeidpour, S.; Corzilius, B. Dynamic Nuclear Polarization for Sensitivity Enhancement in Biomolecular Solid-State NMR. *Chem. Rev.* **2022**, *122*, 9738−9794.

(2) Rossini, A. J.; Zagdoun, A.; Lelli, M.; Lesage, A.; Copéret, C.; Emsley, L. Dynamic Nuclear Polarization Surface Enhanced NMR Spectroscopy. *Acc. Chem. Res.* **2013**, *46*, 1942−1951.

(3) Kobayashi, T.; Perras, F. A.; Slowing, I. I.; Sadow, A. D.; Pruski, M. Dynamic Nuclear Polarization Solid-State NMR in Heterogeneous Catalysis Research. *ACS Catal.* **2015**, *5*, 7055−7062.

(4) Rankin, A. G. M.; Trébosc, J.; Pourpoint, F.; Amoureux, J.-P.; Lafon, O. Recent developments in MAS DNP-NMR of materials. *Solid State Nucl. Magn. Reson.* **2019**, *101*, 116−143.

(5) Maly, T.; Debelouchina, G. T.; Bajaj, V. S.; Hu, K.-N.; Joo, C.-G.; Mak-Jurkauskas, M. L.; Sirigiri, J. R.; van der Wel, P. C. A.; Herzfeld, J.; Temkin, R. J.; Griffin, R. G. Dynamic nuclear polarization at high magnetic fields. *J. Chem. Phys.* **2008**, *128*, No. 052211.

(6) Becerra, L. R.; Gerfen, G. J.; Temkin, R. J.; Singel, D. J.; Griffin, R. G. Dynamic nuclear polarization with a cyclotron resonance maser at 5 T. *Phys. Rev. Lett.* **1993**, *71*, 3561−3564.

(7) Rosay, M.; Tometich, L.; Pawsey, S.; Bader, R.; Schauwecker, R.; Blank, M.; Borchard, P. M.; Cauffman, S. R.; Felch, K. L.; Weber, R. T.; Temkin, R. J.; Griffin, R. G.; Maas, W. E. Solid-state dynamic nuclear polarization at 263 GHz: spectrometer design and experimental results. *Phys. Chem. Chem. Phys.* **2010**, *12*, 5850−5860.

(8) Overhauser, A. W. Polarization of Nuclei in Metals. *Phys. Rev.* **1953**, *92*, 411−415.

(9) Carver, T. R.; Slichter, C. P. Polarization of Nuclear Spins in Metals. *Phys. Rev.* **1953**, *92*, 212−213.

(10) Jeffries, C. D. Polarization of Nuclei by Resonance Saturation in Paramagnetic Crystals. *Phys. Rev.* **1957**, *106*, 164−165.

(11) Abraham, M.; Kedzie, R. W.; Jeffries, C. D. γ-Ray Anisotropy of Co^{60} Nuclei Polarized by Paramagnetic Resonance Saturation. *Phys. Rev.* **1957**, *106*, 165−166.
(12) Hwang, C. F.; Hill, D. A. New Effect in Dynamic Polarization. *Phys. Rev. Lett.* **1967**, *18*, 110−112.
(13) Borghini, M. Spin-Temperature Model of Nuclear Dynamic Polarization Using Free Radicals. *Phys. Rev. Lett.* **1968**, *20*, 419−421.
(14) Wenckebach, W. T. Dynamic nuclear polarization via the cross effect and thermal mixing: A. The role of triple spin flips. *J. Magn. Reson.* **2019**, *299*, 124−134.
(15) Can, T. V.; Ni, Q. Z.; Griffin, R. G. Mechanisms of dynamic nuclear polarization in insulating solids. *J. Magn. Reson.* **2015**, *253*, 23−35.
(16) Hovav, Y.; Feintuch, A.; Vega, S. Theoretical aspects of dynamic nuclear polarization in the solid state−The solid effect. *J. Magn. Reson.* **2010**, *207*, 176−189.
(17) Hovav, Y.; Feintuch, A.; Vega, S. Theoretical aspects of dynamic nuclear polarization in the solid state−The cross effect. *J. Magn. Reson.* **2012**, *214*, 29−41.
(18) Shimon, D.; Hovav, Y.; Feintuch, A.; Goldfarb, D.; Vega, S. Dynamic nuclear polarization in the solid state: a transition between the cross effect and the solid effect. *Phys. Chem. Chem. Phys.* **2012**, *14*, 5729−5743.
(19) Epasto, L. M.; Maimbourg, T.; Rosso, A.; Kurzbach, D. Unified understanding of the breakdown of thermal mixing dynamic nuclear polarization: The role of temperature and radical concentration. *J. Magn. Reson.* **2024**, *362*, No. 107670.
(20) Thurber, K. R.; Tycko, R. Theory for cross effect dynamic nuclear polarization under magic-angle spinning in solid state nuclear magnetic resonance: The importance of level crossings. *J. Chem. Phys.* **2012**, *137*, No. 084508.
(21) Mentink-Vigier, F.; Akbey, Ü.; Hovav, Y.; Vega, S.; Oschkinat, H.; Feintuch, A. Fast passage dynamic nuclear polarization on rotating solids. *J. Magn. Reson.* **2012**, *224*, 13−21.
(22) van Bentum, J.; van Meerten, B.; Sharma, M.; Kentgens, A. Perspectives on DNP-enhanced NMR spectroscopy in solutions. *J. Magn. Reson.* **2016**, *264*, 59−67.
(23) Liu, G.; Levien, M.; Karschin, N.; Parigi, G.; Luchinat, C.; Bennati, M. One-thousand-fold enhancement of high field liquid nuclear magnetic resonance signals at room temperature. *Nat. Chem.* **2017**, *9*, 676−680.
(24) Hope, M. A.; Rinkel, B. L. D.; Gunnarsdóttir, A. B.; Märker, K.; Menkin, S.; Paul, S.; Sergeyev, I. V.; Grey, C. P. Selective NMR observation of the SEI-metal interface by dynamic nuclear polarisation from lithium metal. *Nat. Commun.* **2020**, *11*, 2224.
(25) Miao, Z.; Scott, F. J.; van Tol, J.; Bowers, C. R.; Veige, A. S.; Mentink-Vigier, F. Soliton Based Dynamic Nuclear Polarization: An Overhauser Effect in Cyclic Polyacetylene at High Field and Room Temperature. *J. Phys. Chem. Lett.* **2024**, *15*, 3369−3375.
(26) Can, T. V.; Caporini, M. A.; Mentink-Vigier, F.; Corzilius, B.; Walish, J. J.; Rosay, M.; Maas, W. E.; Baldus, M.; Vega, S.; Swager, T. M.; Griffin, R. G. Overhauser effects in insulating solids. *J. Chem. Phys.* **2014**, *141*, No. 064202.
(27) Ji, X.; Can, T. V.; Mentink-Vigier, F.; Bornet, A.; Milani, J.; Vuichoud, B.; Caporini, M. A.; Griffin, R. G.; Jannin, S.; Goldman, M.; Bodenhausen, G. Overhauser Effects in Non-Conducting Solids at 1.2 K. *J. Magn. Reson.* **2018**, *286*, 138−142.
(28) Pylaeva, S.; Ivanov, K. L.; Baldus, M.; Sebastiani, D.; Elgabarty, H. Molecular Mechanism of Overhauser Dynamic Nuclear Polarization in Insulating Solids. *J. Phys. Chem. Lett.* **2017**, *8*, 2137−2142.
(29) Pylaeva, S.; Marx, P.; Singh, G.; Kühne, T. D.; Roemelt, M.; Elgabarty, H. Organic Mixed-Valence Compounds and the Overhauser Effect in Insulating Solids. *J. Phys. Chem. A* **2021**, *125*, 867−874.
(30) Li, Y.; Equbal, A.; Tabassum, T.; Han, S. ^{1}H Thermal Mixing Dynamic Nuclear Polarization with BDPA as Polarizing Agents. *J. Phys. Chem. Lett.* **2020**, *11*, 9195−9202.
(31) Wenckebach, W. T. Dynamic nuclear polarization via the cross effect and thermal mixing: B. Energy transport. *J. Magn. Reson.* **2019**, *299*, 151−167.
(32) Karabanov, A.; Wiśniewski, D.; Raimondi, F.; Lesanovsky, I.; Köckenberger, W. Many-body kinetics of dynamic nuclear polarization by the cross effect. *Phys. Rev. A* **2018**, *97*, No. 031404.
(33) Hovav, Y.; Kaminker, I.; Shimon, D.; Feintuch, A.; Goldfarb, D.; Vega, S. The electron depolarization during dynamic nuclear polarization: measurements and simulations. *Phys. Chem. Chem. Phys.* **2015**, *17*, 226−244.
(34) Leavesley, A.; Shimon, D.; Siaw, T. A.; Feintuch, A.; Goldfarb, D.; Vega, S.; Kaminker, I.; Han, S. Effect of electron spectral diffusion on static dynamic nuclear polarization at 7 T. *Phys. Chem. Chem. Phys.* **2017**, *19*, 3596−3605.
(35) Kaminker, I.; Shimon, D.; Hovav, Y.; Feintuch, A.; Vega, S. Heteronuclear DNP of protons and deuterons with TEMPOL. *Phys. Chem. Chem. Phys.* **2016**, *18*, 11017−11041.
(36) Kessenikh, A. V.; Lushchikov, V. I.; Manenkov, A. A.; Taran, Y. V. Proton polarization in irradiated polyethylenes. *Sov. Phys. Solid State* **1963**, *5*, 321−329.
(37) Hwang, C. F.; Hill, D. A. Phenomenological Model for the New Effect in Dynamic Polarization. *Phys. Rev. Lett.* **1967**, *19*, 1011−1014.
(38) Serra, S. C.; Rosso, A.; Tedoldi, F. On the role of electron−nucleus contact and microwave saturation in thermal mixing DNP. *Phys. Chem. Chem. Phys.* **2013**, *15*, 8416−8428.
(39) Atsarkin, V. A.; Rodak, M. I. Temperature of Spin-Spin Interactions in Electron Spin Resonance. *Sov. Phys. Uspekhi* **1972**, *15*, 251−265.
(40) Karabanov, A.; Kwiatkowski, G.; Perotto, C. U.; Wiśniewski, D.; McMaster, J.; Lesanovsky, I.; Köckenberger, W. Dynamic nuclear polarisation by thermal mixing: quantum theory and macroscopic simulations. *Phys. Chem. Chem. Phys.* **2016**, *18*, 30093−30104.
(41) Wenckebach, W. T. Electron Spin−Spin Interactions in DNP: Thermal Mixing vs. the Cross Effect. *Appl. Magn. Reson.* **2021**, *52*, 731−748.
(42) Equbal, A.; Li, Y.; Tabassum, T.; Han, S. Crossover from a Solid Effect to Thermal Mixing ^{1}H Dynamic Nuclear Polarization with Trityl-OX063. *J. Phys. Chem. Lett.* **2020**, *11*, 3718−3723.
(43) Quan, Y.; Ouyang, Y.; Mardini, M.; Palani, R. S.; Banks, D.; Kempf, J.; Wenckebach, W. T.; Griffin, R. G. Resonant Mixing Dynamic Nuclear Polarization. *J. Phys. Chem. Lett.* **2023**, *14*, 7007−7013.
(44) Shankar Palani, R.; Mardini, M.; Quan, Y.; Griffin, R. G. Dynamic nuclear polarization with trityl radicals. *J. Magn. Reson.* **2023**, *349*, No. 107411.
(45) Bennati, M.; Luchinat, C.; Parigi, G.; Türke, M.-T. Water ^{1}H relaxation dispersion analysis on a nitroxide radical provides information on the maximal signal enhancement in Overhauser dynamic nuclear polarization experiments. *Phys. Chem. Chem. Phys.* **2010**, *12*, 5902−5910.
(46) Ravera, E.; Luchinat, C.; Parigi, G. Basic facts and perspectives of Overhauser DNP NMR. *J. Magn. Reson.* **2016**, *264*, 78−87.
(47) Levitt, M. H. *Spin Dynamics: Basics for Nuclear Magtnetic Resonance*, 2nd ed.; John Wiley & Sons: West Sussex, U.K., 2008.
(48) Mentink-Vigier; Akbey, Ü; Oschkinat, H.; Vega, S.; Feintuch, A. Theoretical aspects of Magic Angle Spinning - Dynamic Nuclear Polarization. *J. Magn. Reson.* **2015**, *258*, 102−120.
(49) Perras, F. A.; Flesariu, D. F.; Southern, S. A.; Nicolaides, C.; Bazak, J. D.; Washton, N. M.; Trypiniotis, T.; Constantinides, C. P.; Koutentis, P. A. Methyl-Driven Overhauser Dynamic Nuclear Polarization. *J. Phys. Chem. Lett.* **2022**, *13*, 4000−4006.
(50) Heckmann, A.; Lambert, C. Organic Mixed-Valence Compounds: A Playground for Electrons and Holes. *Angew. Chem., Int. Ed.* **2012**, *51*, 326−392.
(51) Wong, K. Y.; Schatz, P. N.; Piepho, S. B. Vibronic coupling model for mixed-valence compounds. Comparisons and predictions. *J. Am. Chem. Soc.* **1979**, *101*, 2793−2803.
(52) Reimers, J. R.; Hush, N. S. Electron transfer and energy transfer through bridged systems. I. Formalism. *Chem. Phys.* **1989**, *134*, 323−354.
(53) Sun, D. L.; Rosokha, S. V.; Lindeman, S. V.; Kochi, J. K. Intervalence (Charge-Resonance) Transitions in Organic Mixed-Valence Systems. Through-Space versus Through-Bond Electron

https://doi.org/10.1021/acs.jpclett.5c00225
J. Phys. Chem. Lett. 2025, 16, 3420−3432

Transfer between Bridged Aromatic (Redox) Centers. *J. Am. Chem. Soc.* **2003**, *125*, 15950−15963.
(54) Uebe, M.; Ito, A. Intramolecular Charge Transfer in Kekulé- and Non-Kekulé-Bridged Bis(triarylamine) Radical Cations: Missing Key Compounds in Organic Mixed-Valence Systems. *Chem.—Asian J.* **2019**, *14*, 1692−1696.
(55) Chevreau, H. Time dependent topological analysis of the electron density in the allyl radical. *Chem. Phys. Lett.* **2004**, *400*, 59−61.
(56) Perras, F. A.; Matsuki, Y.; Southern, S. A.; Dubroca, T.; Flesariu, D. F.; Van Tol, J.; Constantinides, C. P.; Koutentis, P. A. Mechanistic origins of methyl-driven Overhauser DNP. *J. Chem. Phys.* **2023**, *158*, No. 154201.
(57) Hu, K.-N.; Bajaj, V. S.; Rosay, M.; Griffin, R. G. High-frequency dynamic nuclear polarization using mixtures of TEMPO and trityl radicals. *J. Chem. Phys.* **2007**, *126*, No. 044512.
(58) Mathies, G.; Caporini, M. A.; Michaelis, V. K.; Liu, Y.; Hu, K.-N.; Mance, D.; Zweier, J. L.; Rosay, M.; Baldus, M.; Griffin, R. G. Efficient Dynamic Nuclear Polarization at 800 MHz/527 GHz with Trityl-Nitroxide Biradicals. *Angew. Chem., Int. Ed.* **2015**, *54*, 11770−11774.
(59) Wisser, D.; Karthikeyan, G.; Lund, A.; Casano, G.; Karoui, H.; Yulikov, M.; Menzildjian, G.; Pinon, A.; Purea, A.; Engelke, F.; et al. BDPA-Nitroxide Biradicals Tailored for Efficient Dynamic Nuclear Polarization Enhanced Solid-State NMR at Magnetic Fields up to 21.1 T. *J. Am. Chem. Soc.* **2018**, *140*, 13340−13349.
(60) Equbal, A.; Li, Y.; Leavesley, A.; Huang, S.; Rajca, S.; Rajca, A.; Han, S. Truncated Cross Effect Dynamic Nuclear Polarization: An Overhauser Effect Doppelgänger. *J. Phys. Chem. Lett.* **2018**, *9*, 2175−2180.
(61) Shimon, D.; Cantwell, K. A.; Joseph, L.; Williams, E. Q.; Peng, Z.; Takahashi, S.; Ramanathan, C. Large Room Temperature Bulk DNP of ^{13}C via P1 Centers in Diamond. *J. Phys. Chem. C* **2022**, *126*, 17777−17787.
(62) Bussandri, S.; Shimon, D.; Equbal, A.; Ren, Y.; Takahashi, S.; Ramanathan, C.; Han, S. P1 Center Electron Spin Clusters Are Prevalent in Type Ib Diamonds. *J. Am. Chem. Soc.* **2024**, *146*, 5088−5099.
(63) Tobar, C.; Albanese, K.; Chaklashiya, R.; Equbal, A.; Hawker, C.; Han, S. Multi Electron Spin Cluster Enabled Dynamic Nuclear Polarization with Sulfonated BDPA. *J. Phys. Chem. Lett.* **2023**, *14*, 11640−11650.
(64) Radaelli, A.; Yoshihara, H. A. I.; Nonaka, H.; Sando, S.; Ardenkjaer-Larsen, J. H.; Gruetter, R.; Capozzi, A. ^{13}C Dynamic Nuclear Polarization using SA-BDPA at 6.7 T and 1.1 K: Coexistence of Pure Thermal Mixing and Well-Resolved Solid Effect. *J. Phys. Chem. Lett.* **2020**, *11*, 6873−6879.
(65) Mandal, S.; Sigurdsson, S. T. On the Limited Stability of BDPA Radicals. *Chem.—Eur. J.* **2020**, *26*, 7486−7491.
(66) Azuma, N.; Ozawa, T.; Yamauchi, J. Molecular and Crystal Structures of Complexes of Stable Free Radical BDPA with Benzene and Acetone. *Bull. Chem. Soc. Jpn.* **1994**, *67*, 31−38.
(67) Müllegger, S.; Rashidi, M.; Fattinger, M.; Koch, R. Interactions and Self-Assembly of Stable Hydrocarbon Radicals on a Metal Support. *J. Phys. Chem. C* **2012**, *116*, 22587−22594.
(68) Müllegger, S.; Rashidi, M.; Fattinger, M.; Koch, R. Surface-Supported Hydrocarbon π Radicals Show Kondo Behavior. *J. Phys. Chem. C* **2013**, *117*, 5718−5721.
(69) Sato, H.; Kathirvelu, V.; Spagnol, G.; Rajca, S.; Rajca, A.; Eaton, S. S.; Eaton, G. R. Impact of Electron−Electron Spin Interaction on Electron Spin Relaxation of Nitroxide Diradicals and Tetraradical in Glassy Solvents Between 10 and 300 K. *J. Phys. Chem. B* **2008**, *112*, 2818−2828.
(70) Chaklashiya, R. K.; Equbal, A.; Shernyukov, A.; Li, Y.; Tsay, K.; Stern, Q.; Tormyshev, V.; Bagryanskaya, E.; Han, S. Dynamic Nuclear Polarization Using Electron Spin Cluster. *J. Phys. Chem. Lett.* **2024**, *15*, 5366−5375.
(71) Salikhov, K. M.; Dzuba, S. A.; Raitsimring, A. M. The theory of electron spin-echo signal decay resulting from dipole-dipole interactions between paramagnetic centers in solids. *J. Magn. Reson.* **1981**, *42*, 255−276.
(72) Equbal, A.; Ramanathan, C.; Han, S. Dipolar Order Induced Electron Spin Hyperpolarization. *J. Phys. Chem. Lett.* **2024**, *15*, 5397−5406.
(73) Caracciolo, F.; Filibian, M.; Carretta, P.; Rosso, A.; De Luca, A. Evidence of spin-temperature in dynamic nuclear polarization: an exact computation of the EPR spectrum. *Phys. Chem. Chem. Phys.* **2016**, *18*, 25655−25662.
(74) Wenckebach, W. T. Spectral diffusion and dynamic nuclear polarization: Beyond the high temperature approximation. *J. Magn. Reson.* **2017**, *284*, 104−114.
(75) Corzilius, B.; Smith, A. A.; Griffin, R. G. Solid effect in magic angle spinning dynamic nuclear polarization. *J. Chem. Phys.* **2012**, *137*, No. 054201.
(76) Mance, D.; Gast, P.; Huber, M.; Baldus, M.; Ivanov, K. L. The magnetic field dependence of cross-effect dynamic nuclear polarization under magic angle spinning. *J. Chem. Phys.* **2015**, *142*, No. 234201.
(77) Mentink-Vigier, F.; Vega, S.; De Paëpe, G. Fast and accurate MAS−DNP simulations of large spin ensembles. *Phys. Chem. Chem. Phys.* **2017**, *19*, 3506−3522.
(78) Mentink-Vigier, F.; Mathies, G.; Liu, Y.; Barra, A.-L.; Caporini, M. A.; Lee, D.; Hediger, S.; Griffin, R. G.; De Paëpe, G. Efficient cross-effect dynamic nuclear polarization without depolarization in high-resolution MAS NMR. *Chem. Sci.* **2017**, *8*, 8150−8163.
(79) Gurinov, A.; Sieland, B.; Kuzhelev, A.; Elgabarty, H.; Kühne, T. D.; Prisner, T.; Paradies, J.; Baldus, M.; Ivanov, K. L.; Pylaeva, S. Mixed-Valence Compounds as Polarizing Agents for Overhauser Dynamic Nuclear Polarization in Solids. *Angew. Chem., Int. Ed.* **2021**, *60*, 15371−15375.
(80) Hu, K.-N.; Debelouchina, G. T.; Smith, A. A.; Griffin, R. G. Quantum mechanical theory of dynamic nuclear polarization in solid dielectrics. *J. Chem. Phys.* **2011**, *134*, No. 125105.
(81) Delage-Laurin, L.; Palani, R. S.; Golota, N.; Mardini, M.; Ouyang, Y.; Tan, K. O.; Swager, T. M.; Griffin, R. G. Overhauser Dynamic Nuclear Polarization with Selectively Deuterated BDPA Radicals. *J. Am. Chem. Soc.* **2021**, *143*, 20281−20290.
(82) Palani, R. S.; Mardini, M.; Delage-Laurin, L.; Banks, D.; Ouyang, Y.; Bryerton, E.; Kempf, J. G.; Swager, T. M.; Griffin, R. G. Amplified Overhauser DNP with Selective Deuteration: Attenuation of Double-Quantum Cross-Relaxation. *J. Phys. Chem. Lett.* **2023**, *14*, 95−100.
(83) Maly, T.; Cui, D.; Griffin, R. G.; Miller, A.-F. ^{1}H Dynamic Nuclear Polarization Based on an Endogenous Radical. *J. Phys. Chem. B* **2012**, *116*, 7055−7065.
(84) Edmondson, D. E. Electron-spin-resonance studies of flavoenzymes. *Biochem. Soc. Trans.* **1985**, *13*, 593−600.
(85) Martínez, J. I.; Alonso, P. J.; Gómez-Moreno, C.; Medina, M. One- and Two-Dimensional ESEEM Spectroscopy of Flavoproteins. *Biochem.* **1997**, *36*, 15526−15537.
(86) García, J. I.; Medina, M.; Sancho, J.; Alonso, P. J.; Gómez-Moreno, C.; Mayoral, J. A.; Martínez, J. I. Theoretical Analysis of the Electron Spin Density Distribution of the Flavin Semiquinone Isoalloxazine Ring within Model Protein Environments. *J. Phys. Chem. A* **2002**, *106*, 4729−4735.
(87) Weber, S.; Möbius, K.; Richter, G.; Kay, C. W. M. The Electronic Structure of the Flavin Cofactor in DNA Photolyase. *J. Am. Chem. Soc.* **2001**, *123*, 3790−3798.
(88) Martínez, J. I.; Alonso, P. J.; García-Rubio, I.; Medina, M. Methyl rotors in flavoproteins. *Phys. Chem. Chem. Phys.* **2014**, *16*, 26203−26212.
(89) Benetis, N. P.; Zelenetckii, I. A.; Dmitriev, Y. A. Low-temperature tunneling of CH3 quantum rotor in van der Waals solids. *Low Temp. Phys.* **2019**, *45*, 427−440.
(90) Wind, R. A.; Bai, S.; Hu, J. Z.; Solum, M. S.; Ellis, P. D.; Grant, D. M.; Pugmire, R. J.; Taylor, C. M. V.; Yonker, C. R. ^{1}H Dynamic Nuclear Polarization in Supercritical Ethylene at 1.4 T. *J. Magn. Reson.* **2000**, *143*, 233−239.

https://doi.org/10.1021/acs.jpclett.5c00225
J. Phys. Chem. Lett. 2025, 16, 3420−3432